Science Advances
AAAS

advances.sciencemag.org/cgi/content/full/6/5/eaay2739/DC1

Supplementary Materials for

The physiological effects of noninvasive brain stimulation fundamentally differ across the human cortex

Gabriel Castrillon, Nico Sollmann, Katarzyna Kurcyus, Adeel Razi, Sandro M. Krieg, Valentin Riedl*

*Corresponding author. Email: valentin.riedl@tum.de

Published 31 January 2020, *Sci. Adv.* **6**, eaay2739 (2020)
DOI: 10.1126/sciadv.aay2739

This PDF file includes:

Table S1. Participants demographic information and individual TMS target coordinates in MNI space.
Table S2. Statistical significant changes in whole-brain functional connectivity after OCC-TMS as presented in Fig. 2 and fig. S2A.
Table S3. Statistical significant changes in whole-brain functional connectivity after FRO-TMS as presented in Fig. 2 and fig. S2B.
Fig. S1. Image quality assessment.
Fig. S2. Cross-sectional representation of Fig. 2A.
Fig. S3. Statistical significance of the modularity results.
Fig. S4. Classification results using linear support vector machine (SVM).
Fig. S5. Effect of the parameter τ on the global functional integration results.

Supplementary Materials

Table S1. Participants demographic information and individual TMS target coordinates in MNI space.

ID	sex	age(y)	FRO-target(mm)			OCC-target(mm)			CTR-target(mm)		
			x	y	z	x	y	z	x	y	z
sub-s001	F	26	-51.52	46.90	26.68	-12.93	-109.64	-12.79	-80.66	-54.01	9.72
sub-s002	F	23	-45.64	49.89	18.81	-12.39	-110.44	-12.74	-70.33	-59.69	12.58
sub-s003	M	23	-54.43	36.78	35.78	-10.46	-111.14	-16.66	-74.42	-59.83	11.53
sub-s004	F	23	-44.73	37.20	51.19	-17.63	-113.67	-16.75	-79.04	-59.41	13.17
sub-s005	F	27	-41.30	37.53	44.18	-6.25	-126.79	-10.17	-79.80	-47.59	30.98
sub-s006	F	25	-58.13	38.07	27.08	-3.92	-118.12	-9.65	-76.84	-59.93	9.72
sub-s007	M	28	-50.54	35.55	39.01	-16.21	-120.43	1.93	-77.65	-61.20	27.38
sub-s008	F	25	-45.97	32.21	50.71	-18.58	-116.44	-19.12	-79.64	-61.81	9.08
sub-s009	F	29	-50.56	44.44	30.41	-6.54	-120.67	-13.07	-78.43	-59.60	12.53
sub-s010	M	25	-42.80	56.83	25.20	-10.06	-121.21	-5.96	-68.31	-64.45	15.30
sub-s011	F	30	-52.32	54.43	7.82	-6.49	-121.30	-16.86	-80.53	-62.90	12.21
sub-s012	M	26	-42.97	40.20	41.84	-17.30	-124.90	-6.41	-72.50	-65.07	12.56
sub-s013	F	19	-43.33	33.27	39.30	-17.81	-112.89	-17.34	-72.83	-62.94	11.17
sub-s014	F	32	-50.76	42.64	38.81	-11.91	-119.81	-17.77	-82.06	-63.49	7.59
sub-s015	M	24	-48.06	38.74	46.13	-20.85	-116.41	-14.13	-81.09	-62.64	9.38
sub-s016	F	22	-56.33	38.14	34.31	-7.53	-113.87	-14.61	-73.62	-63.83	13.03
sub-s017	M	29	-51.13	49.41	28.17	-14.92	-123.81	-11.45	-83.82	-57.27	11.14
sub-s018	M	31	-44.06	48.06	26.84	-19.42	-118.17	-16.29	-76.38	-59.62	8.69
sub-s019	M	22	-48.36	45.02	41.23	-22.20	-111.86	-17.16	-74.90	-59.68	12.57
sub-s020	F	25	-47.81	40.97	39.58	-17.77	-112.83	-23.58	-78.38	-58.38	10.68
sub-s021	M	23	-42.59	44.05	37.46	-18.66	-119.60	-13.12	-73.88	-58.65	11.99
sub-s022	M	28	-42.67	41.78	37.08	-12.45	-119.41	-11.44	-77.03	-59.60	11.53
sub-s023	M	27	-41.28	45.85	36.80	-15.27	-109.27	-13.91	-74.46	-62.84	10.22

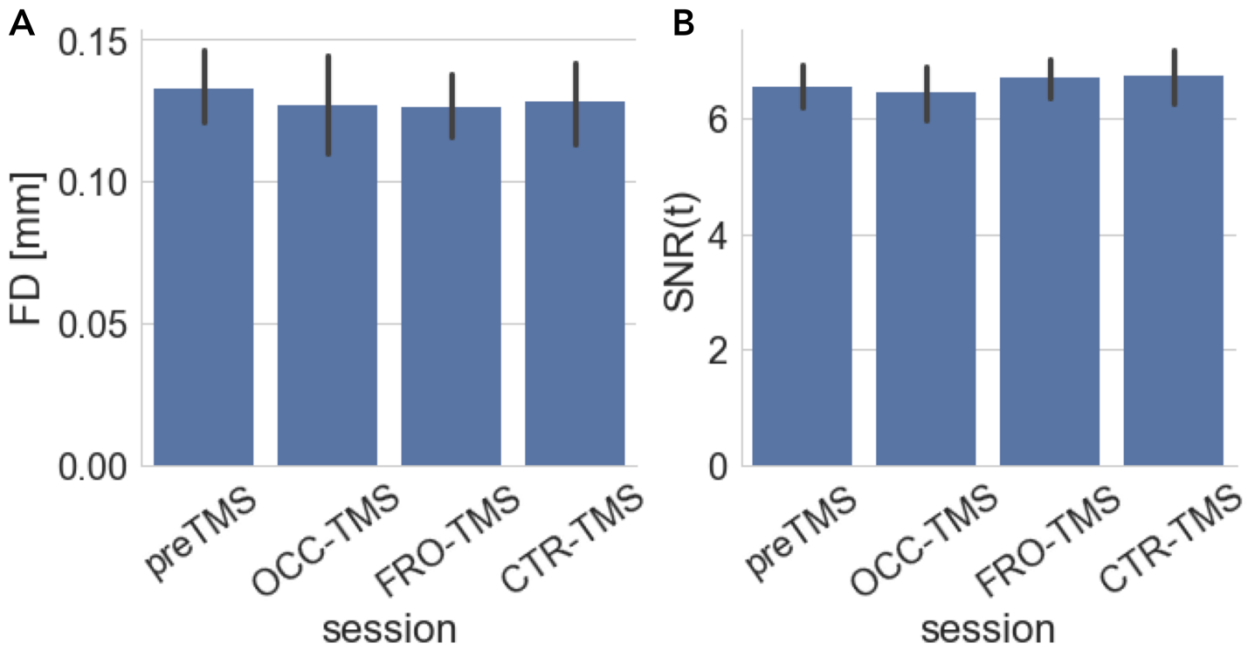

Fig. S1. Image quality assessment. Bar plots represent (**A**) framewise displacement (FD) and (**B**) temporal SNR (SNR(*t*)) across TMS sessions. Error bars represent the 95% confidence interval of variance across subjects. Overall, there were not significant differences for any of the two parameters across TMS sessions ($p > 0.05$, repeated measures ANOVAs).

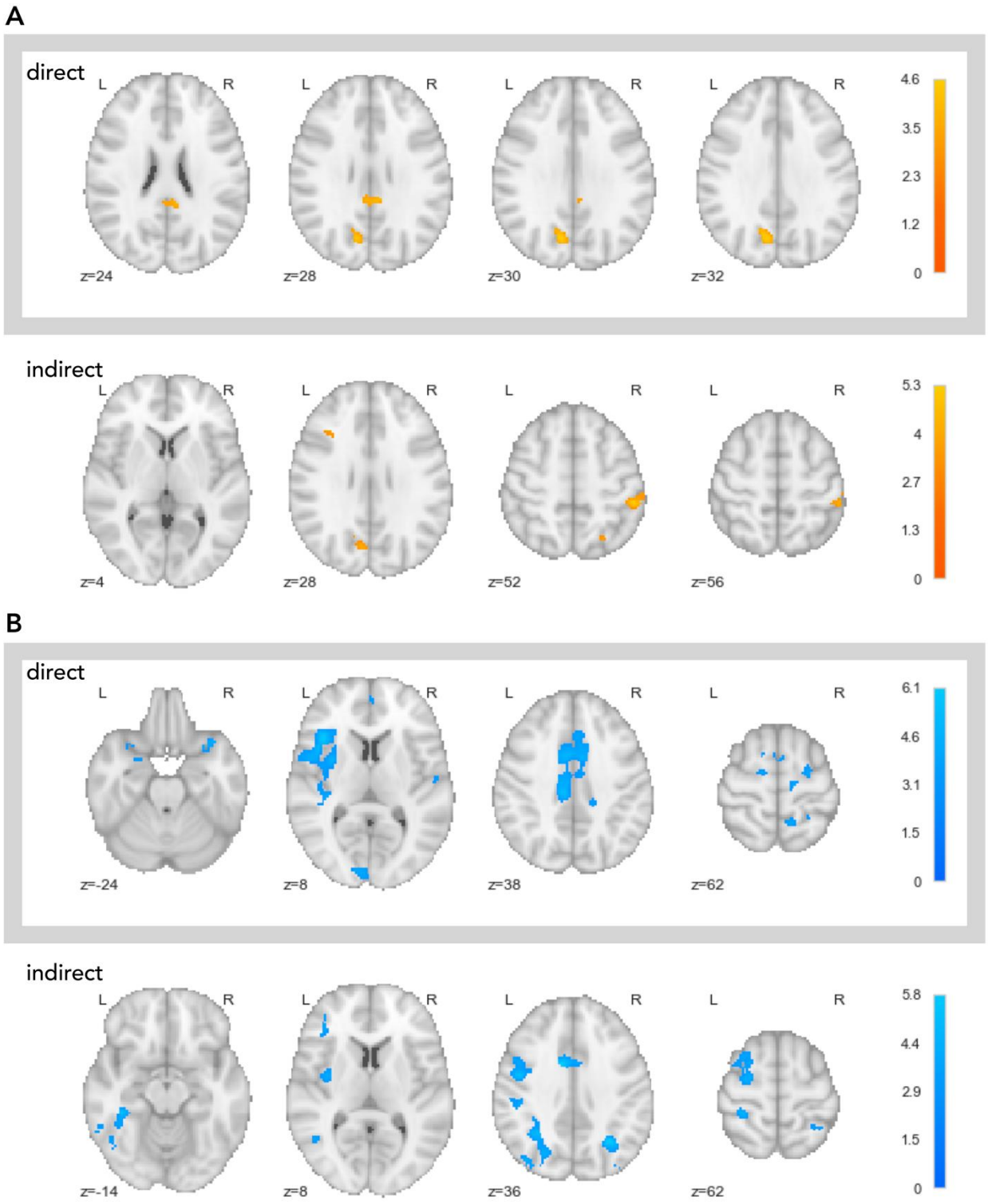

Fig. S2. Cross-sectional representation of Fig. 2A. Statistical parametric maps of significant changes in whole-brain functional connectivity after OCC- (**A**) and FRO- (**B**) TMS (pFWE < 0.05, corrected at cluster level, voxel-wise repeated measures ANOVAs).

Table S2. Statistical significant changes in whole-brain functional connectivity after OCC-TMS as presented in Fig. 2 and fig. S2A. Anatomical locations derived from the Harvard-Oxford structural atlas. Acronyms: PCG, posterior cingulate gyrus; PCUN, precuneus; FP, frontal pole； MFG, middle frontal gyrus; IPL, inferior parietal lobule; IPS, intraparietal sulcus; PCG, posterior cingulate gyrus.

Direct									
Cluster			**Peak**			**MNI(mm)**			**Region**
p(FWE)	**p(unc)**	**k(vox)**	**p(FWE)**	**p(unc)**	**T**	**x**	**y**	**z**	
0	0	242	0.158	0	5.16	8	-38	28	PCG
			0.954	0	4.21	-4	-38	28	
			0.962	0	4.19	-4	-24	28	
0	0	181	0.21	0	5.06	-10	-70	30	PCUN
			1	0	3.67	14	-60	32	
Indirect									
0	0	357	0.092	0	5.33	-10	68	18	FP
			0.27	0	4.96	-42	50	10	
			0.7	0	4.53	-24	64	16	
0	0	422	0.129	0	5.22	-6	-72	32	PCUN
			0.819	0	4.41	-18	-54	16	
			0.893	0	4.32	-12	-64	20	
0.001	0	145	0.209	0	5.05	-48	10	42	MFG
			0.999	0	3.92	-46	12	50	
0.001	0	139	0.231	0	5.02	48	-34	52	R IPL
0	0	494	0.237	0	5.01	-36	-38	44	L aIPS
			0.44	0	4.77	-42	-30	42	
			0.986	0	4.09	-44	-38	54	
0.003	0	115	0.688	0	4.54	-30	-80	40	L IPL
			0.985	0	4.1	-42	-72	38	
			1	0	3.66	-38	-80	36	
0	0	242	0.861	0	4.36	14	-60	32	PCUN
			0.947	0	4.22	8	-44	22	
			0.997	0	3.96	14	-54	24	
0.001	0	150	0.862	0	4.36	-30	18	34	MFG
			0.977	0	4.13	-46	22	32	
			0.999	0	3.92	-36	28	22	
0	0	269	0.927	0	4.26	38	-70	40	R IPL
			0.961	0	4.19	30	-72	40	
			0.977	0	4.13	24	-66	50	

0	0	163	0.929	0	4.26	-6	-44	14	PCG
			0.999	0	3.92	-6	-36	30	
			1	0	3.63	-6	-42	22	

Table S3. Statistical significant changes in whole-brain functional connectivity after FRO-TMS as presented in Fig. 2 and fig. S2B. Anatomical locations derived from the Harvard-Oxford structural atlas. Acronyms: AIC, anterior insular cortex; dACC, dorsal anterior cingulate cortex; SPL, superior parietal lobule; MTG middle temporal gyrus; SFG superior frontal gyrus.

Direct									
Cluster			**Peak**			**MNI(mm)**			**Region**
p(FWE)	**p(unc)**	**k(vox)**	**p(FWE)**	**p(unc)**	**T**	**x**	**y**	**z**	
0	0	845	0.05	0	5.52	-50	12	-2	L AIC
			0.1	0	5.3	-40	22	8	
			0.982	0	4.11	-32	4	8	
0	0	954	0.303	0	4.92	-10	6	50	dACC
			0.324	0	4.89	-2	16	28	
			0.462	0	4.75	-10	6	36	
0	0	227	0.925	0	4.27	14	-46	56	R SPL
			0.978	0	4.13	20	-50	52	
			0.999	0	3.92	16	-42	48	
0.007	0	102	0.999	0	3.89	-10	-24	38	L SPL
			1	0	3.85	-12	-14	38	
Indirect									
0.001	0	133	0.188	0	5.1	28	-60	36	R IPS
0	0	186	0.736	0	4.5	-46	-4	38	PreCG
			0.974	0	4.15	-46	4	30	
0	0	545	0.765	0	4.47	-30	-66	30	L IPS
			0.871	0	4.36	-34	-52	52	
			0.981	0	4.12	-34	-54	36	
0	0	155	0.853	0	4.38	-58	-48	-8	MTG
			0.991	0	4.06	-50	-58	-16	
			1	0	3.82	-50	-50	-4	
0.006	0	102	0.892	0	4.33	-20	14	50	SFG
			0.999	0	3.94	-26	8	50	
			1	0	3.82	-20	0	52	
0.005	0	104	0.958	0	4.2	-34	4	58	MFG
			0.994	0	4.03	-26	-8	62	
			1	0	3.52	-30	-4	52	

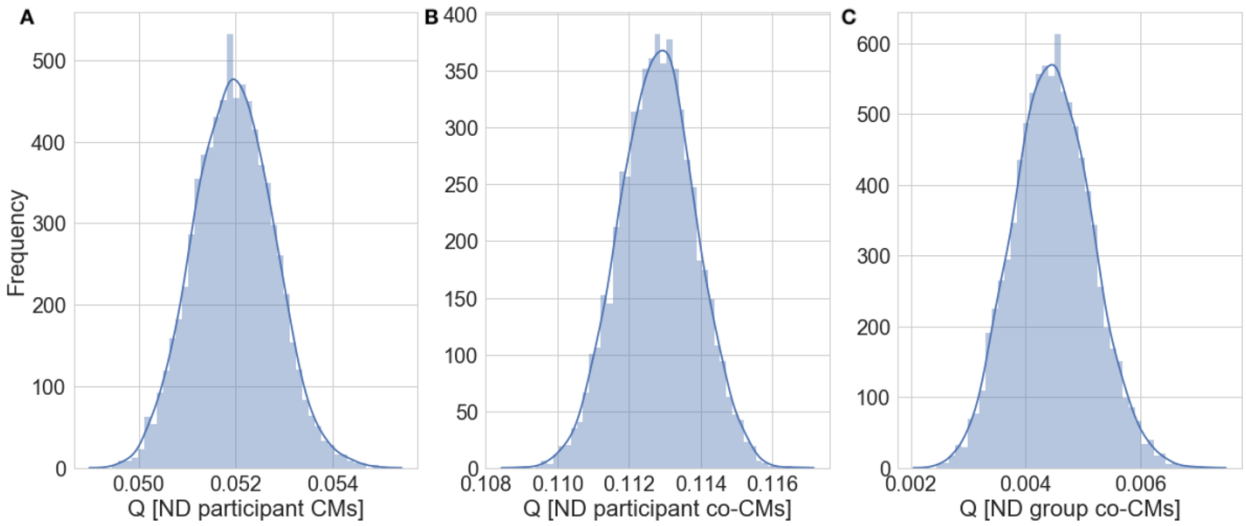

Fig. S3. Statistical significance of the modularity results. Null model distributions (ND) of median Q values based on (**A**) the individual functional connectivity matrices, (**B**) the individual co-classification matrices, and (**C**) the group co-classification matrices. The modularity results were more modular than expected by chance when compared to the null model for the individual connectivity matrices (Q_{pre} = 0.181, Q_{OCC} = 0.143, Q_{FRO} = 0.165; p < 0.001, permutation testing), individual co-classification matrices (Q_{pre} = 0.585, Q_{OCC} = 0.544, Q_{FRO} = 0.588; *p* < 0.001, permutation testing) and group co-classification matrices (Q_{pre} = 0.266, Q_{OCC}= 0.244, Q_{FRO} = 0.274; *p* < 0.001, permutation testing).

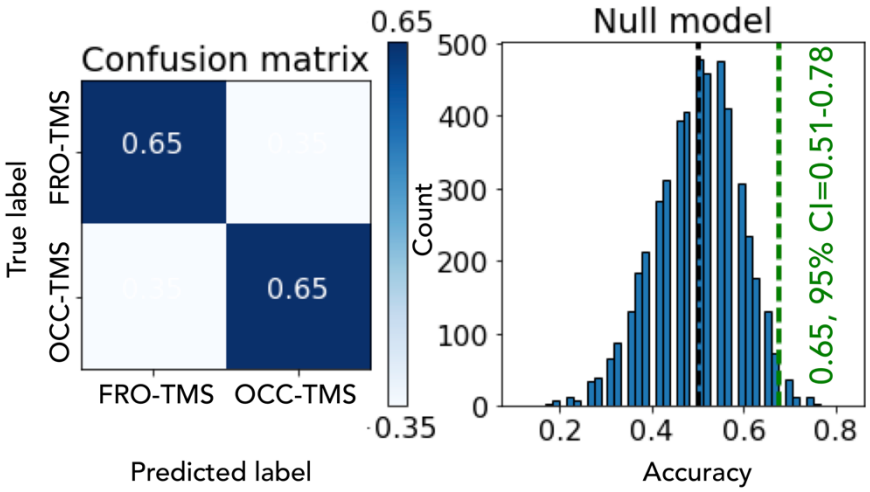

Fig. S4. Classification results using linear support vector machine (SVM). Results of classification between VIS- and SAL-TMS data lead to a 65% prediction accuracy. (Left) Confusion matrix with the prediction accuracies for every class and (Right) null distribution of chance after 5000 permutations which shows that our results are significantly higher than chance (p = 0.029, permutation testing).

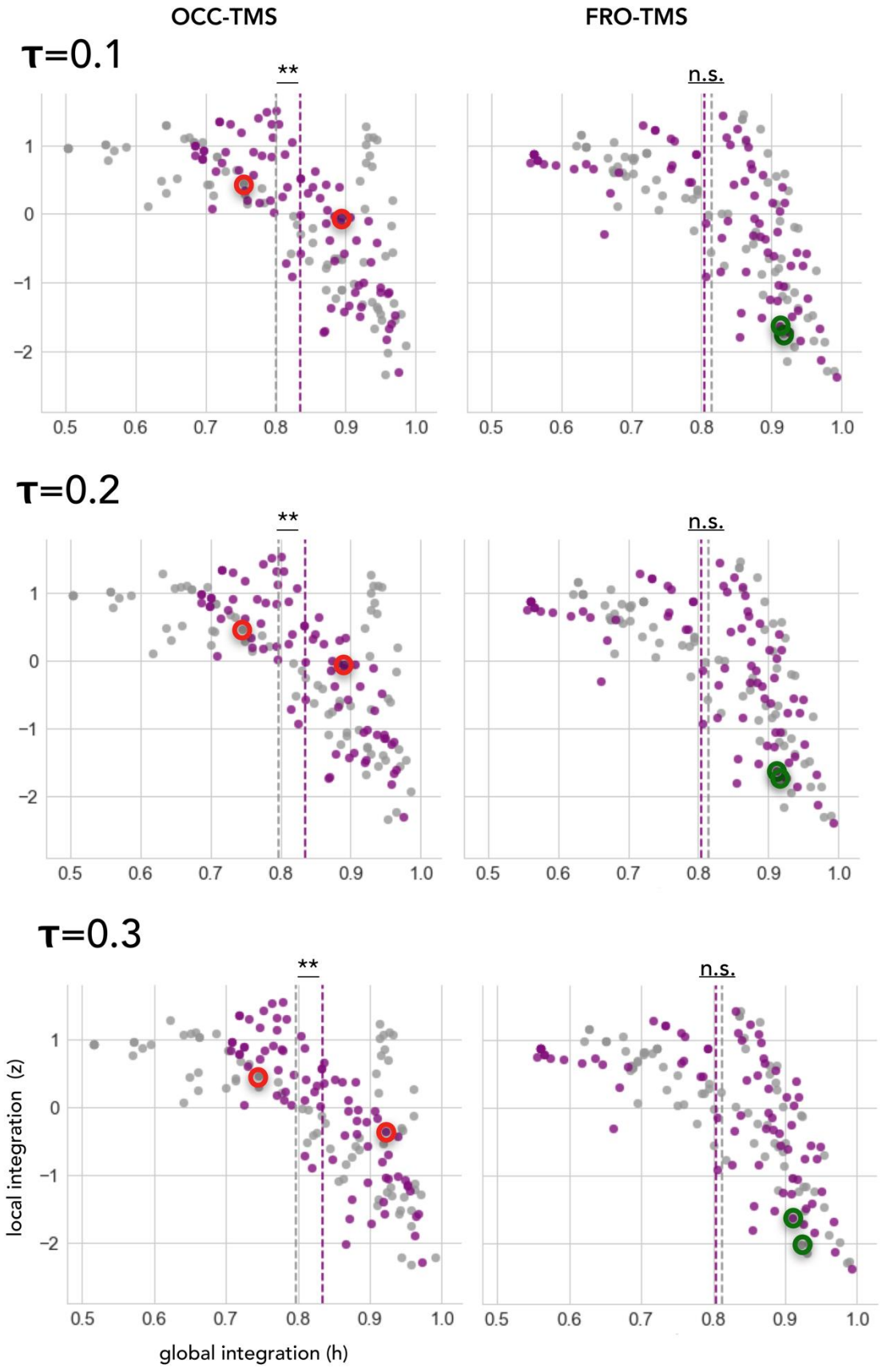
OCC-TMS
FRO-TMS
τ=0.1
**
n.s.
τ=0.2
**
n.s.
τ=0.3
**
n.s.
local integration (z)
global integration (h)
1
0
−1
−2
0.5
0.6
0.7
0.8
0.9
1.0

Fig. S5. Effect of the parameter τ on the global functional integration results. Scatterplots of z vs. h before (grey) and after (violet) stimulation across the range of optimal values for the consensus modularity parameter τ ($\tau \leq 0.4$), which reproduces the global functional integration results obtained using the recommended value of $\tau = 0.4$ (57) in (Fig. 3C-D). ** $p < 0.01$, Wilcoxcon signed-rank test.